Arch. Min. Sci. **68** (2023), 4, 671-684

Electronic version (in color) of this paper is available: http://mining.archives.pl

DOI: https://doi.org/10.24425/ams.2023.148156

WEIDONG YU[1*]

EXPERIMENTAL STUDY OF LIGNITE STRUCTURE EVOLUTION CHARACTERISTICS AND MECHANISMS UNDER THERMAL-MECHANICAL CO-FUNCTION

In-situ thermal upgrading modification technology is of great significance to lignite utilisation cleanly. It is an extremely complex multi-field coupling process. Therefore, it is necessary to study the physical properties of lignite under the thermo-mechanical coupling function. In this paper, the lignite pore evolution characteristics under thermal-mechanical co-function have been obtained at different scales based on experimental results. The mechanisms also have been deeply studied. The results indicated that lignite total porosity first increased and then decreased as the temperature increased from 23°C to 400°C under the triaxial stress of 7 MPa. The maximum value of 21.64% for the total porosity of lignite was observed at 200°C. Macropores were dominant when the temperature was lower than 100°C, while visible pores were dominant when at temperatures ranging from 100~400°C. The thermal weight loss and deformation characteristics of lignite were further studied using a thermal-mechanical testing platform. The weight loss and deformation process could be divided into three stages, namely the slow, rapid, and relatively slow stages. After being continuously pyrolysed for 5 hours at a temperature of 400°C, the maximum weight loss rate of lignite was 52.38%, the maximum axial linear strain was 11.12%, and the maximum irrecoverable radial strain was 18.79%. The maximum axial thermal deformation coefficient of lignite was -2.63×10^{-4} °C^{-1} at a temperature of 289°C. Macro-deformation and component loss were the main mechanisms of lignite structure evolution.

Keywords: Mechanism; lignite; deformation; thermal-mechanical co-function; structure evolution

1. Introduction

Lignite plays a crucial role in the energy structure of the world [1-3]. However, due to the high moisture, high ash and low calorific value of lignite, the lignite is mostly open-pit mined [4,5] and is utilised after ground upgrading and modification. The mining and utilisation of

[1] SHANXI INSTITUTE OF ENERGY, CHINA

* Corresponding author: yuwd@sxie.edu.cn

lignite will seriously endanger the environment, such as surface damage and air pollution. To address these problems, a new comprehensive method of in situ superheated steam injection and fluidised mining was proposed and has become widely accepted [6-8]. In the process of in situ fluidised mining, coal is subjected to a coupled thermal and mechanical environment. Hence, the pores and fissures of coal evolve significantly [9,10]. However, pores and fissures are important indexes that reflect the macromechanical properties of materials (including the elasticity modulus, permeability, and fracture behaviour) [11-13]. Hence, an in-depth understanding of the structure evolution characteristics of lignite under coupled temperature and stress with superheated steam injection becomes necessary.

At present, the main methods for analysing coal and rock structures in laboratories include computed tomography [14], mercury injection testing, liquid nitrogen adsorption analysis, NMR, SEM, optical microscopy and MS/AE source location method [15]. A large amount of experimental data indicates that the influence of temperature on pore and fissure characteristics is mainly due to thermal fracturing at lower temperatures and thermal pyrolysis at high temperatures. For example, at room temperature, the characteristics of pores and fissures vary with coal metamorphism. In terms of the degree of pore development, anthracite is ranked first, followed by lignite and then bitumite, while lignite outranks anthracite and both outrank bitumite in terms of the degree of heterogeneity [16]. For lean coal, the porosity slowly decreases from room temperature to 200°C while the porosity sharply increases from 200 to 400°C. The porosity of lean coal quickly decreases from 400 to 600°C. In addition, the diameter of the largest pore or fissure increases with increasing temperature [17].

For soft coal, when the temperature rises, the microcrack extension rate first increases and then decreases, and the extension rate of cracks parallel to the bedding direction is greater than for those perpendicular to the bedding direction [18]. Furthermore, as the temperature rises, sub micropores are gradually transformed into other types of pores, and the overall meso-physical parameters and fractal dimensions of the specimen first decrease and then increase with increasing temperature [19].

The mechanic state is another important factor that can contribute greatly to coal structure evolution. For example, the porosity of subbituminous coal decreases with increasing pyrolysis pressure, and the diameter of the main pores and fissures ranges from 300 to 5000 nm [20]. Confining pressure has a certain inhibitory effect on the development of fractures in coal and also has effects on the forms and spatial distribution features of failure fractures in coal [21]. During the process of in situ thermal fluidisation mining, coal is under the coupled action of ground stress, temperature, and moisture. Thus, the evolution of pores and fissures is largely affected by macro-deformation and composition evolution. In addition, the deformation characteristics of coal are affected by mechanical parameters such as Young's modulus and the effective stress level of coal [22,23], while the composition evolution is primarily influenced by the temperature field, product retention time, and pyrolysis atmosphere [24,25]. However, these experimental results have certain limitations because the test methods and experimental parameters cannot precisely reflect the actual in situ state of coal.

Previously, researchers have concentrated on coal characteristics under chemical or physical environments, while there are few reports on the evolution characteristics of pores and fissures, which range from micro- to macro size, under the coupled action of a multiphysical field. In this paper, the pore and fissure evolution characteristics of lignite under the triaxial stress condition of 7 MPa within 400°C were studied in depth at multiple scales using micro-CT method, mercury

injection testing, and liquid nitrogen adsorption-desorption testing. The liquid nitrogen testing is used to analyse the evolution characteristics of pores and fractures less than 25 nm. The Mercury injection testing is used to analyse the evolution characteristics of pores and fractures between 25 nm and 100 um. And Micro-CT method is used to analyse the evolution characteristics of pores and fractures larger than 100 um. Further, the deformation and thermal weight loss characteristics of lignite were also studied using a thermal-mechanical testing platform. Thus, the structure evolution mechanism of lignite was determined. This research is of great significance to the further development of technologies in energy utilisation.

2. Experiment parameters and test procedure

2.1. Experimental setup

The comprehensive testing platform used in this study is composed of a superheated steam generating device and thermal-mechanical testing platform (as shown in Fig. 1). The experimental temperature ranged from 23°C to 400°C. The steam pressure ranged from 0.1 to 20 MPa. The tested temperature and pressure conditions are outlined in TABLE 1.

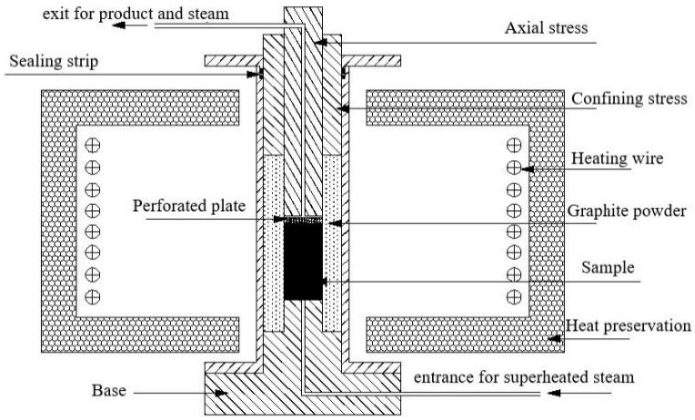

Fig. 1. The thermal-mechanical testing platform

The maximum magnification of micro-CT is 400× with a maximum image resolution of 5.24×104 PPI. In our experiments, lignite samples were observed at 7.31× magnification, and images were acquired at a resolution of 957.4 PPI.

The measurable pressure of the Mercury Injection Instrument (Pore Master 33) ranged from 1.5 KPa to 231 MPa (0.2-33,000 PSI), and the measurable pore diameter ranged from 7 nm to 1000 μm. All of the testing samples used in mercury injection testing were dewatered for 24 h at 80°C in a nitrogen atmosphere before being tested.

The instrument used in our experiments for liquid nitrogen adsorption was a NOVA 2000E. The diameter of the samples ranged from 0.2 to 0.5 mm. The testing samples were also dewatered for 24 h at 80°C in a nitrogen atmosphere in advance.

TABLE 1

The sample information

	Serial number	Length (mm)	Diameter (mm)	Quality (g)	Magnification times	Temperature (℃)	Axle pressure (MPa)	Confining pressure (MPa)
Micro-CT Method	1#	103.20	50.11	240.75	7.31	100	7	7
	3#	102.07	49.97	240.17	7.31	200	7	7
	17#	103.76	49.58	239.23	7.31	300	7	7
	25#	97.50	49.80	234.92	7.31	400	7	7

	Serial number	Volume (mL)	Quality (g)		Serial number	Quality (g)
Mercury Injection Testing	1#	0.79	0.6307	**Liquid Nitrogen Adsorption Testing**	1#	3.8277
	3#	0.81	0.8323		3#	3.9202
	17#	1.08	1.2201		17#	4.5724
	25#	1.11	1.3628		25#	4.4827

2.2. Sample information

All samples were taken from the fifth coal seam of the Datang open pit lignite mine, Xilinhaote, Inner Mongolia Autonomous Region. The results for coal analysis of lignite are shown in TABLE 2. The samples tested in the thermal-mechanical and micro-CT experiments were 50 mm in diameter and 100 mm in length. A hole, approximately 3 mm in diameter, was drilled straight through the centre of the sample. For steam flow, a stainless steel pipe with a diameter of about 3 mm and holes on the lateral surface is pre-placed in the sample (stress state of coal samples as shown in Fig. 2 and Fig. 3). The samples indicated above were used for mercury injection and liquid nitrogen adsorption testing.

TABLE 2

Coal analysis of samples

Proximate analysis				Elemental analysis				
FCad	**Mad**	**Aad**	**Vad**	**C**	**H**	**O**	**N**	**S**
41.24%	9.93%	9.23%	39.6%	60.2%	4.24%	13.44	0.8%	2.16%

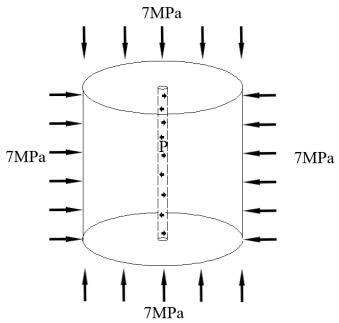

Fig. 2. The stress state of the lignite samples

Original sample pyrolysis at 100°C Original sample pyrolysis at 200°C

Original sample pyrolysis at 300°C Original sample pyrolysis at 400°C

Fig. 3. Lignite samples

2.3. Experimental procedures

(1) Lignite original structure testing: Analysis of lignite original structure characteristics was obtained by using the micro-CT method, mercury injection testing and liquid nitrogen adsorption testing.

(2) Triaxial stress applied process: The original lignite samples were placed in the thermal-mechanical testing platform. The axle stress and confining stress were alternately increased to 7 MPa step by step. Then, the stress was stably maintained for 3 hours to ensure that there was no decrease in stress. The axle stress was obtained by rigid loading, while the stress transmitting medium of the confining stress was flaky graphite powder.

(3) Air exhaust process: The air in the experimental system was cleanly pumped out via the injection of distilled water, and this process lasted for approximately 1.5 hours.

(4) Heating process: The temperature of the lignite sample was increased to the experimental temperatures (100, 200, 300, and 400°C) from 23°C at a rate of 3°C/min, and the axle displacement of the sample was measured every minute.

(5) Keep temperature and stress stable: Stable stress and temperature were maintained for 300 minutes, and the axle displacement of the lignite sample was obtained every minute.
(6) Analysis of experimented lignite: We removed the tested sample, and the thermal weight loss was analysed by balance; the structure characteristics were also analysed using the micro-CT method, mercury injection testing and liquid nitrogen adsorption testing.

3. Results and analysis

3.1. Lignite pore and fissure evolution characteristics

The structure evolution characteristics of lignite after being pyrolyzed for 5 hours are shown in Figs. 4-6 below.

Original sample

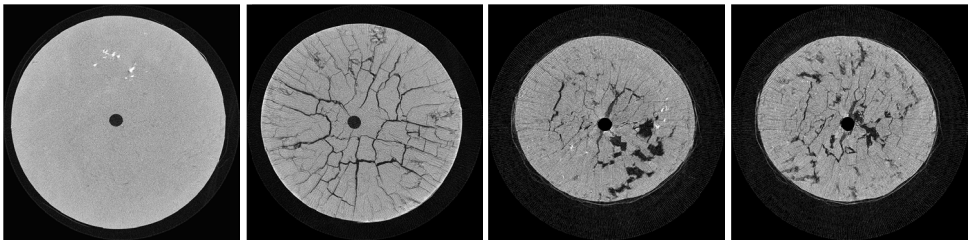

100℃ 200℃ 300℃ 400℃

Fig. 4. Micro-CT images of lignite at different temperatures

It can be concluded from Fig. 4 that the original lignite sample is dense. At 100℃, there is no obvious change in the lignite sample. At 200℃, a lot of large pore cracks were observed, and the lignite has undergone significant compression deformation. With the temperature increased lots of pyrolysis holes were observed while the number of pore cracks decreased. Further, the significant radial compression deformation was visible in the lignite sample.

The mercury injection testing results indicated that the pore cracks in lignite are mainly concentrated above 10um and below 0.1um. With the temperature increase, the pores of different scales have undergone significant evolution. Further analysis was necessary to study the pore evolution characteristics at different scales.

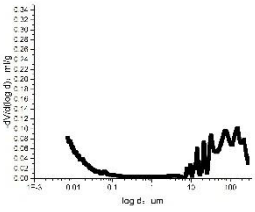

Original sample

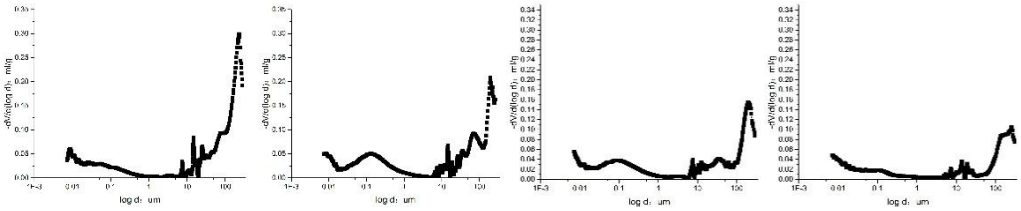

100℃ 200℃ 300℃ 400℃

Fig. 5. Results of the mercury injection testing

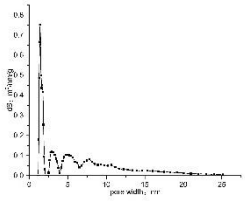

Original sample

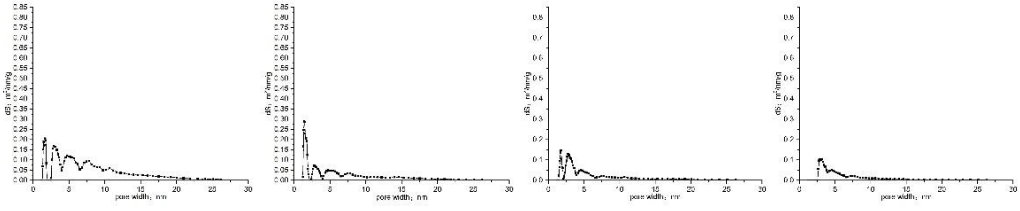

100℃ 200℃ 300℃ 400℃

Fig. 6. Results of the liquid nitrogen adsorption testing

Based on the liquid nitrogen adsorption testing results, it can be confirmed that the nm-level pores of lignite are mainly concentrated below 5 nm. With the temperature increase, the pores with a diameter less than 5 nm gradually decrease.

Based on the results, the structure evolution characteristics of lignite under thermal and mechanical co-function were obtained, as shown in Fig. 7 below. In this paper, the B.B. Hodort [26] pore classification method is mainly adopted. The pores larger than 100 um are subdivided into two types: macropores (1-100 μm) and viewable pores (larger than 100 μm).

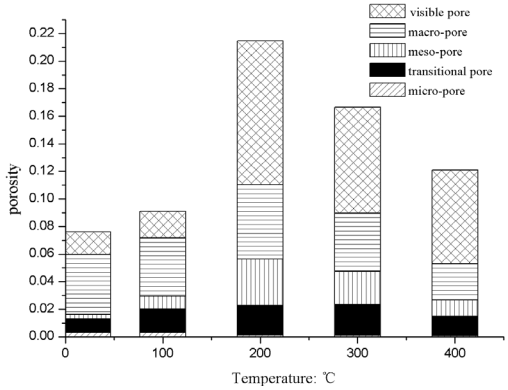

Fig. 7. The evolution of pores and fissures according to different scales

As shown in Fig. 7, the total porosity of lignite under triaxial stress first increased and then decreased with increasing temperature. The total porosity of the original lignite sample was only approximately 7.6%, which was the lowest observed value. After being pyrolyzed for 5 hours in a 100°C steam atmosphere, the total porosity of the lignite sample increased smoothly to 9.11% with an increasing amplitude of 1.51%. When the temperature increased to 200°C, the total porosity rapidly increased to 21.45% with an increasing amplitude of 13.85%. However, the total porosity suddenly decreased to 16.64% as the temperature continued to rise to 300°C. Similarly, at 400°C, the total porosity of lignite continuously decreased to 12.08% with a decreasing amplitude of 4.56%.

The evolution characteristics of different scales of pores and fissures were studied, as shown in Fig. 7. In this paper, the pores and fissures were differentiated according to diameter as micropores (less than 10 nm), transitional pores (10-100 nm), mesopores (100-1000 nm), macropores (1-100 μm), and viewable pores (larger than 100 μm). The results indicate that the largest total volume observed within 100°C corresponded to macropores, while viewable pores were the main type of pore in the lignite structure at higher temperatures. Micropores accounted for the lowest proportion of the lignite structure according to volume within 400°C. When the temperature increased, the porosity of micropores decreased gradually from 0.33% at 23°C to 0.08% at 400°C. However, the porosities of the transitional pores, mesopores, macropores, and viewable pores all first increased and then decreased. The transitional temperature of the transitional pores was 300°C with a porosity of 2.23%, while the transitional temperatures of the mesopores, macropores, and viewable pores were all 200°C with a porosity of 3.35%, 5.42%, and 10.42% respectively. When the temperature increased, the percentage values of transitional pore and mesopore increased and then decreased. The percentage of macropores was demonstrated to gradually decrease from 57.39% at 23°C to 22.04% at 400°C while the percentage of viewable pores gradually increased from 21.31% at 23°C to 56.1% at 400°C according to volume.

3.2. Weight loss characteristics of lignite with increasing temperature

The curve for weight loss with increasing temperature was obtained, as shown in Fig. 8. The results indicate that the weight loss process of lignite when the temperature is increased

to 400°C can be divided into three stages, the slow weight loss stage, when the temperature is increased from 23°C to 100°C, the rapid weight loss stage, when the temperature was increased from 100 to 300°C, and the relatively slow weight loss stage when the temperature was increased from 300 to 400°C. The weight loss characteristics indicate that the weight loss of lignite would result in the lignite macro-deformation process under thermal-mechanical co-function.

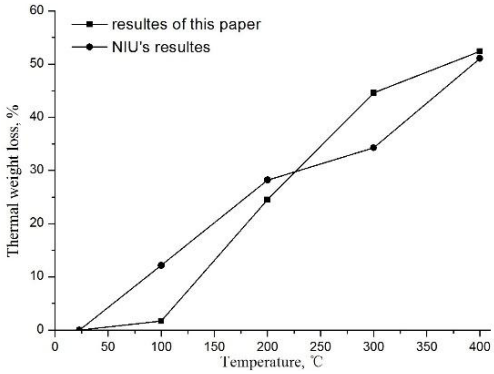

Fig. 8. Weight loss characteristics of lignite

The main influences of temperature on coal are the dewatering function within 120°C, the degassing function (CH_4, CO_2, and N_2) within 200°C, the decarboxylation reaction with temperatures higher than 200°C, and the thermolysis function with temperatures higher than 300°C [27]. As the NIU's results show in Fig. 8 [28], without stress loading, the weight loss of lignite would rapidly increase when the temperature increased from 23 to 200°C, then slowly increase when the temperature increased from 200 to 300°C and, finally, quickly increase again when the temperature increased from 300 to 400°C. These thermal weight loss characteristics show good agreement with the conclusions of Xie [27]. However, our results indicate that the thermal weight loss with stress loading was completely different. The results of our experiments indicate that the thermal weight loss process under stress loading was delayed. The moisture and adsorbed gas were more difficult to precipitate because the lignite structure became more compact under stress loading, and the thermolysis process was also delayed.

3.3. Deformation characteristics of lignite with increasing temperatures

The deformation characteristics of lignite were obtained for increases in temperature from 23°C to 400°Cas shown in Fig. 9.

As shown in Fig. 9, the axial deformation process of lignite can be divided into three stages. The first stage is the slow swelling stage when the temperature is increased from 23 to 170°C. In this stage, the axial thermal strain of lignite was shown to be increasing in a near-linear fashion. The axial thermal expansion coefficient ranged from 1.4×10^{-5} to $1.5\times10^{-5}\,°C^{-1}$, and the average value was $1.47\times10^{-5}\,°C^{-1}$. The deformation characteristics can be explained as Equation (1), in which T stands for the temperature value. The value of Adj. R-Square is 0.992.

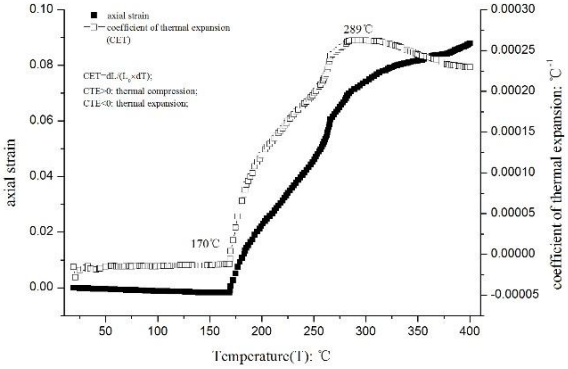

Fig. 9. The axial deformation characteristics of lignite

$$\varepsilon = 1.2509\times10^{-5}T - 1.033\times10^{-4}(18°C \le T \le 170°C) \quad (1)$$

The second stage is the rapidly compressing stage when the temperature increases from 170 to 289°C. In this stage, the axial thermal deformation quickly turns from the swelling state to the compressing state. The axial strain rapidly increased from -6.15×10^{-4} to -7.14×10^{-2}. Similarly, the axial thermal expansion coefficient rapidly increased from -4.02×10^{-6} to -2.63×10^{-4} °C^{-1}. The deformation characteristics can be explained as Equation (2). The value of Adj. R-Square is 0.99.

$$\varepsilon = -5.7067\times10^{-4}T + 0.0938\,(170°C < T < 289°C) \quad (2)$$

The third stage is the relatively slow compressing stage when the temperature increases from 289 to 400°C. In this stage, the axial strain rate was smaller than the rapidly compressing stage but larger than the slow swelling stage. The axial thermal expansion coefficient smoothly decreased from -2.63×10^{-4} to -2.3×10^{-4} °C^{-1}. An obvious strain-hardening phenomenon was observed in this stage. The deformation process of this stage can be explained as Equation (3). The value of Adj. R-Square is 0.969.

$$\varepsilon = 1.2347\times10^{-4}T - 0.0383\,(289°C \le T \le 400°C) \quad (3)$$

To further study the mechanism of lignite deformation, both the lignite weight loss characteristics and structural evolution under thermal-mechanical co-function were analysed. At the same time, the total radial strain and total volume strain were determined using software from the micro-CT images after the samples were stably heated for 300 min in a pyrolysis reaction device at the tested temperatures. The radial deformation, which is analysed by calculating the equivalent diameter of micro-CT images along with the total axial strain and total volume strain was obtained, as shown in Fig. 10.

The results indicate that the total radial strain was increasing nearly linearly when the temperature increased from 100 to 400 °C. The deformation process can be obtained by Equation (4).

$$\varepsilon_{total} = 0.06177\,T - 6.125(100°C \le T \le 400°C) \quad (4)$$

The value of Adj. R-Square is 0.999. However, the total axial strain showed a different trend. The total axial strain of lignite first increased from 2.01% to 10.17% when the temperature increased from 100 to 200°C, and then smoothly increased from 10.17% to 11.12% when the

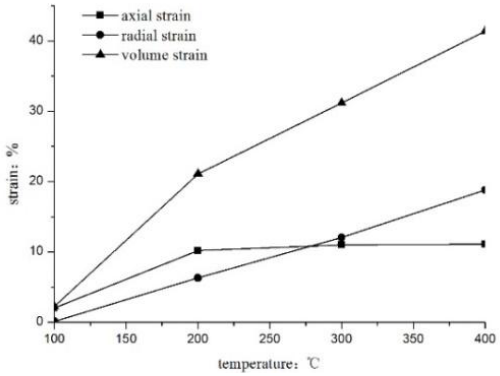

Fig. 10. Accumulative deformation under different temperatures

temperature increased from 200 to 400°C. Similarly, the total volume strain also first increased rapidly and then slowly increased. Therefore, the total radial strain showed an increasing contribution as the temperature increased.

4. Discussion

As a kind of special porous media, the structure evolution characteristics of lignite under thermal and mechanical co-function have been proven to be different from other rocks, such as granite [29], shale [30], and glauberite [31]. This is mainly determined by the evolution of coal composition and macro deformation under the co-functions of temperature and mechanics.

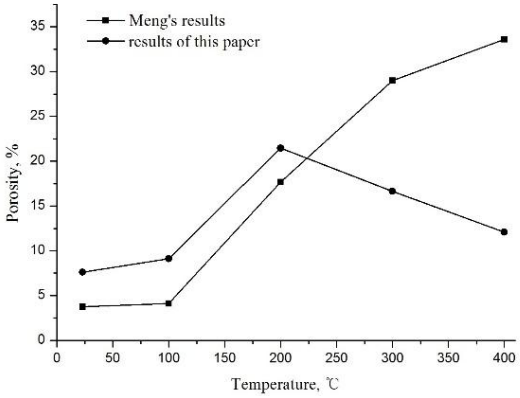

Fig. 11. Total porosity of lignite with increasing temperatures

First, when the temperature increased, the lignite structure significantly changed with the dewatering function, degassing function, and complex pyrolysis reaction. When the coal components were dissimilar, there were clear differences in the pores and fissures after coal pyrolysis.

Without stress, the coal pyrolysis process can be divided into three stages within 400°C [27]. These are the dehydration process with temperatures below 120°C, the degassing process with temperatures below 200°C (mainly CH_4, CO_2, and N_2), and the pyrolytic polymerisation/thermal decomposition reaction with temperatures ranging from 300 to 400°C. This indicates that the lignite pores and fissures evolve with changing temperatures. The smaller the pore or fissure size and the poorer the connectivity of coal, the longer the migration time of the pyrolysis products in coal. Then, the coal pyrolysis characteristics differ from those of better permeability, resulting in a different coal structure.

While under the effect of stress, the pores and fissures collapse or close, especially the macropores and viewable pores. The physical and mechanical properties of coal are changed along with the evolution of coal pores and fissures under thermal and mechanical co-function. As shown in Fig. 11, without triaxial stress, the total lignite porosity increased smoothly when the temperature increased from 23 to 100°C. Then, it rapidly increased at higher temperatures. However, the porosity increased smoothly again if the temperature exceeded 300°C [32]. Under the triaxial stress of 7 MPa, the evolution characteristic of porosity was the same as that of lignite under no triaxial stress within 200°C. When the temperature was higher than 200°C, clear differences between the two porosity values were obtained. The total porosity of the lignite sample without triaxial stress continuously increased, while that of the lignite sample with 7 MPa triaxial stress decreased.

The distribution characteristics of the pores and fissures at different scales were also studied. The results indicate that the scale of the main pores and fissures decreased when the temperature increased under no triaxial stress. At 100°C, the pores and fissures above 800 μm were dominant. At 200°C, the pores and fissures ranging from 100 to 800 μm dominated. The pores and fissures smaller than 100 μm were dominant if the temperature was higher than 300°C. However, the scale of the main pores and fissures gradually increased when the temperature increased under 7 MPa triaxial stress. The percentage of pores and fissures less than 25 nm decreased, while that of pores and fissures ranging from 25 nm to 1 μm increased when the temperature increased. The critical transition temperature was approximately 200°C. The percentage of pores and fissures ranging from 1 to 100 μm gradually decreased while that of pores and fissures larger than 100 μm gradually increased.

The results also indicate that the lignite component changed from a physical phase transition (for example, water changing from liquid to gaseous phase or adsorbed gas changing from adsorbed to free phase) to chemical thermolysis. The mechanism of structure evolution changed from thermal fracture to pyrolysis. Furthermore, under thermal and mechanical coupling effects, the mechanical properties were weakened; the coal changed from brittle to plastic, and the deformation became more severe. With the compression, closure, and collapse of the pores and fissures, the lignite structure changed and returned to being relatively compact with the occurrence of a strain-hardening stage. In conclusion, changes in components and macro deformation were identified in this study as the key factors underlying the structure evolution characteristics of lignite under thermal-mechanical co-functions.

5. Conclusions

In this paper, the evolution characteristics of lignite pores and fissures at different scales under coupled thermal-mechanical stress were extensively studied using micro-CT method,

mercury injection testing and liquid nitrogen adsorption-desorption testing. The mechanism of lignite structure evolution was also discussed. Our main conclusions are as follows.

(1) Under the action of coupled temperature and stress, the total porosity of lignite first increased and then decreased with pyrolysis with increasing temperatures. The porosity was 7.6% at 23°C, 9.11% at 100°C, 21.45% at 200°C, 16.64% at 300°C, and 12.09% at 400°C.
(2) When the temperature was lower than 100°C, the total volume was dominated by macropores while visible pores were dominant, according to volume, when the temperature ranged from 100 to 400°C.
(3) The weight loss of lignite under coupled thermal-mechanical stress as the temperature increased from 23°C to 400°C was shown to consist of three stages, which are the slow, rapid, and relatively slow weight loss stages.
(4) The axial deformation characteristics of lignite under the coupled action of thermal and mechanical stress occurred in three stages, which are the slowly swelling, rapidly compressing, and relatively slowly compressing stages. The critical transition temperatures were 170 and 289°C. The critical temperature of the brittle–ductile transition of lignite was approximately 180°C. A distinct strain hardening stage was observed at temperatures higher than 300°C.

Acknowledgement

The research was supported by, Science and Technology Major Project in Shanxi (20191102002), Scientific and Technological Innovation Programs of High Educations Institutions in Shanxi (2019L0990), and Shanxi Province Natural Science Foundation (20210302124489).

References

[1] X.H. Fu, L. Lu, Y.Y. Ge, J.J. Tian, P.P. Luo, China Lignite Resources and Physical Features. Coal Science and Technology **40**, 10, 104-107+112 (2012).

[2] V.Ș. Ediger, I. Berk Kösebalaban A, Lignite resources of Turkey: Geology, reserves, and exploration history. International Journal of Coal Geology **132**,13-22 (2014).

[3] A. Tajduś ,S. Tokarski, Risks related to energy policy of Poland until 2040 (EPP 2040). Archives of Mining Sciences **65**, 4, 877-899 (2020).

[4] D. Vrublová, R. Kapica, S. Smelik, M. Smeliková, Real-time positioning of equipment and material tracking of waste streams in surface coal mining – a case study. Archives of Mining Sciences **66**, 2, 249-264 (2021).

[5] S.M. Pathan, A.G. Pathan, F.I. Siddiqui, M.B. Memon, M.H.A.A. Soomro, Open pit slope stability analysis in soft rock formations at Thar coalfield Pakistan. Archives of Mining Sciences **67**, 3, 437-454 (2022).

[6] Y.S. Zhao, Multi-field coupling action and engineering response of porous media. Beijing: Science Press, 2010.

[7] Y.S. Zhao, F. Qu, Z.J. Wan, Y. Zhang, W.G. Liang, Q.R. Meng, Experimental Investigation on Correlation Between Permeability Variation and Pore Structure During Coal Pyrolysis. Transport in Porous Media **82**, 2, 401-412 (2009).

[8] H.P. Xie, Y. Ju, M.Z. Gao, F. Gao, J.Z. Liu, H.W. Ren, S.R. Ge, Theories and technologies for in-situ fluidized mining of deep underground coal resources. Journal of China Coal Society **43**, 5, 1210-1219 (2018).

[9] Y.M. Yu, Y.Q. Hu, W.G. Liang, Q.R. Meng, Z.C. Feng, Study on pore characteristics of lean coal at different temperature by CT technology. Chinese Journal of Geophysics **55**, 2, 637-644 (2012).

[10] Z.X. Mi, F.G. Wang, N. Shi, J.Z. Yu, Z.J. Sun, Experimental study on effect of multi-stage stress variations on permeability and pore structure of sandstone. Chinese Journal of Geotechnical Engineering **43**, 5, 1210-1219 (2018).

[11] Z.J. Wu, L.F. Fan, Q.S. Liu, G.W. Ma, Micro-mechanical modeling of the macro-mechanical response and fracture behavior of rock using the numerical manifold method. Engineering Geology **225**, 49-60 (2017).

[12] S.W. Niu, Y.S. Zhao, Y.Q. Hu, Experimental Investigation of the Temperature and Pore Pressure Effect on Permeability of Lignite Under the In Situ Condition. Transport in Porous Media **101**, 1, 137-148 (2013).

[13] L. Zhang, S. Chen, C. Zhang, X.Q. Fang, S. Li, The characterization of bituminous coal microstructure and permeability by liquid nitrogen fracturing based on μCT technology. Fuel **262**, 116635 (2020).

[14] G.L. Zhang, P.G. Ranjith, H.E. Huppert, Direct evidence of coal swelling and shrinkage with injecting CO2 and N2 using in-situ synchrotron xray microtomography, Engineering **18**, 11, 88-95 (2022).

[15] L.J. Dong, Q.C. Hu, X.J. Tong,Y.F. Liu, Velocity-free MS/AE source location method for three-dimensional hole-containing structures. Engineering **6**, 7, 827-834 (2020).

[16] Y. Sun, C. Zhai, J.Z. Xu, L. Qin, W. Tang, A method for accurate characterisation of the pore structure of a coal mass based on two-dimensional nuclear magnetic resonance T1-T2. Fuel **262**, 116574 (2020).

[17] Y.M. Yu, W.G. Liang, Y.Q. Hu, Q.R. Meng, Study of micro-pores development in lean coal with temperature. International Journal of Rock Mechanics and Mining Sciences **51**, 91-96 (2012).

[18] Q.R. Meng, Y.S. Zhao, Y.M. Yu, Y.Q. Hu, Micro-CT experimental study of crack evolution of lignite under different temperatures. Chinese Journal of Rock Mechanics and Engineering **29**, 12, 2475-2483 (2010).

[19] T. Meng, J.L. Xie, X.M. Li, J.W. Ma, Y. Yang, Experimental study on the evolutional trend of pore structures and fractal dimension of low-rank coal rich clay subjected to a coupled thermo-hydro-mechanical-chemical environment. Energy **203**, 117838 (2020).

[20] J. Tomeczek, S. Gil, Volatiles release and porosity evolution during high pressure coal pyrolysis. Fuel **82**, 285-292 (2003).

[21] Y.Y. Li, H.Q. Cui, P. Zhang, D.K. Wang, J.P. Wei, Three-dimensional visualization and quantitative characterization of coal fracture dynamic evolution under uniaxial and triaxial compression based on μCT scanning. Fuel **262**, 116568 (2020).

[22] Z.J. Feng, Z.J. Wan, Y.S. Zhao, G.W. Li, Y. Zhang, C. Wang, Experimental investigation into deformation characteristics of anthracite under thermal-mechanical coupling conditions. Chinese Journal of Rock Mechanics and Engineering **29**, 08, 1624-1630 (2010).

[23] Z.J. Wan, Z.J. Feng, Y.S. Zhao, Y. Zhan, G.W. Li,C.B. Zhou, Elastic modulus's evolution law of coal under high temperature and triaxial stress. Journal of China Coal Society **36**, 10, 1736-1740 (2011).

[24] J.T. Zhang, R.K. Shi, B. Niu, H.Q. Hu, S.R. Liang, H.B. Zhong, Effect of CH4 atmosphere on tar yield and quality in coal pyrolysis at low-medium pyrolysis temperature. Journal of China Coal Society **46**, 1, 292-299 (2021).

[25] Q. Zhou, Experimental study on the pyrolysis of Xinjiang Naomaohu coal in a moving bed with baffled internals. Journal of China Coal Society **46**, 12, 4054-4062 (2021).

[26] B.B. Hodot, S.Z. Song, Y.A. Wang, Outburst of coal and coalbed gas. Beijing: China Industry Press (1966).

[27] K.C. Xie, Coal structure and its reactivity. Beijing: Science Press (2002).

[28] S.W. Niu, Investigation of Pyrolysis and Thermostatic Weight Loss Properties of Lignite. Coal Technology **34**, 12, 263-264 (2015).

[29] D.J. Xue, B. Hu, Y. Fang, Z. Zhuo, H.W. Zhou, Paths on thermal-mechanical coupling failure of meso-scale granite under uni-axial tension and numerical analysis. Journal of China Coal Society **41**, 09, 2212-2222 (2016).

[30] Y.D. Geng, W.G. Liang, J. Liu, Z.Q. Kang, P.F. Wu, Y.L. Jiang, Experimental study on the variation of pore and fracture structure of oil shale under different temperatures and pressures. Chinese Journal of Rock Mechanics and Engineering **37**, 11, 2510-2519 (2018).

[31] Q. Qian, Mechanical property weakening and micro structure evolution of glauberite under different leaching temperature [Dissertation]. Taiyuan University of Technology, P.30, 2017.

[32] Q.R. Meng, Y.S. Zhao, Y.Q. Hu, Z.C. Feng, S.G. Xu, Micro-CT experimental of the thermal cracking of brown coal. Journal of China Coal Society **36**, 05, 855-860 (2011).